Biomaterials 72 (2015) 152–162

Contents lists available at ScienceDirect

Biomaterials

journal homepage: www.elsevier.com/locate/biomaterials

Homogeneous generation of iDA neurons with high similarity to *bona fide* DA neurons using a drug inducible system

Hanseul Park [a, 1], Hongwon Kim [a, 1], Junsang Yoo [a, 1], Jaekwang Lee [c], Hwan Choi [a], Soonbong Baek [a], C. Justin Lee [c], Janghwan Kim [d], Christopher J. Lengner [b], Jung-Suk Sung [e], Jongpil Kim [a, *]

[a] *Lab of Stem Cells & Cell Reprogramming, Department of Biomedical Engineering, Dongguk University, Seoul, 100-715, Republic of Korea*
[b] *Department of Animal Biology, School of Veterinary Medicine, University of Pennsylvania, Philadelphia, PA, 19104, USA*
[c] *Center for Neural Science and Functional Connectomics, Brain Science Institute, Korea Institute of Science and Technology, Seoul, 136-791, Republic of Korea*
[d] *Stem Cell Research Center, Korea Research Institute of Bioscience and Biotechnology (KRIBBB), Korea University of Science & Technology (UST), Daejeon 305-333, Republic of Korea*
[e] *Department of Life Science, Dongguk University, Seoul, 100-715, Republic of Korea*

ARTICLE INFO

Article history:
Received 8 July 2015
Received in revised form
31 August 2015
Accepted 3 September 2015
Available online 6 September 2015

Keywords:
Direct lineage reprogramming
Gene expression system
Induced neurons

ABSTRACT

Recent work generating induced dopaminergic (iDA) neurons using direct lineage reprogramming potentially provides a novel platform for the study and treatment Parkinson's disease (PD). However, one of the most important issues for iDA-based applications is the degree to which iDA neurons resemble the molecular and functional properties of their endogenous DA neuron counterparts. Here we report that the homogeneity of the reprogramming gene expression system is critical for the generation of iDA neuron cultures that are highly similar to endogenous DA neurons. We employed an inducible system that carries iDA-inducing factors as defined transgenes for direct lineage reprogramming to iDA neurons. This system circumvents the need for viral transduction, enabling a more efficient and reproducible reprogramming process for the generation of genetically homogenous iDA neurons. We showed that this inducible system generates iDA neurons with high similarity to their *bona fide in vivo* counterparts in comparison to direct infection methods. Thus, our results suggest that homogenous expression of exogenous genes in direct lineage reprogramming is critical for the generation of high quality iDA neuron cultures, making such culture systems a valuable resource for iDA-based drug screening and, ultimately, potential therapeutic intervention in PD.

1. Introduction

Recently, we and others have reported that mouse and human fibroblasts can be directly reprogrammed into different subtypes of neurons, including dopamine (DA) neurons, by viral transduction of specific transcription factors [1–5]. Generation of induced dopamine (iDA) neurons from abundant somatic cells make this system attractive for autologous cell based therapies because this approach can eliminate the necessity of passing through the pluripotent state and subsequent directed differentiation inherent in ES or iPS cell-based approaches [6]. Furthermore, direct lineage conversion eliminates the potential for undifferentiated pluripotent cells to form teratomas upon transplantation. Thus, the generation of iDA neurons has significant implications for the potential direct therapeutic use in Parkinson's disease (PD) and, in the near-term, has immediate applicability as an *in vitro* screening platform for the identification of small molecules targeting PD.

Previous studies characterizing iDA neurons revealed a number of differences in their molecular features when compared to primary DA neurons, with iDA neurons showing close similarity and some shared functional features of mesencephalic DA neurons [3–5,7]. Similarly, the functional efficacy of iDA neurons upon *in vivo* transplantation is lower than those of primary midbrain DA neurons [3]. One possible reason for these differences is the degree

* Corresponding author. Dept of Biomedical Engineering, Dongguk University, Seoul, Korea.
E-mail addresses: jk2316@gmail.com, jpkim153@dongguk.edu (J. Kim).
[1] These authors are equally contributed.

http://dx.doi.org/10.1016/j.biomaterials.2015.09.002
0142-9612/

of heterogeneity within iDA cultures with respect to the number of cells that receive the proper dosage or optimal stoichiometric ratios of reprogramming factors for precise lineage conversion. This heterogeneity largely results from viral site-of-integration effects and insertion frequency and likely contributes to incomplete reprogramming and/or low reprogramming efficiency. The precedent for this phenomenon is abundant in the field of induced pluripotency [8–10]. Thus, cellular and genetic heterogeneity associated with direct conversion complicates the potential application of iDA neurons in PD drug screening and, ultimately, in cell replacement therapy.

Much effort has been applied to the development of new methods to overcome the challenges associated with the generation of induced cells. For example, expression of Lmx1a/Fox2a in ES/iPSCs or fibroblasts has been shown to lead to the efficient generation of DA neurons [11], decreasing complications associated with heterogeneity for the therapeutic application of DA neurons. Additionally, Tian et al. recently showed the generation of directly converted DA precursors [12], which resulted in the specific DA neuronal lineage, possibly supplying a reasonable source of cells for PD treatment. Moreover, several small molecules or engineered substrates that can improve DA neurons efficiency and quality have been identified [13–15]. Nevertheless, the low efficiency and heterogeneity of DA neurons still remains as a significant barrier in the safe and efficient DA neuron-based cell replacement for PD.

Thus, in this study, to test whether the quality and efficiency of iDA neuron generation can be improved by a homogenous factor expression system, we established an inducible system to homogenously generate iDA neurons directly from somatic cells. Analogous strategies in inducible pluripotency reprogramming systems have proven to be more efficient and synchronous than reprogramming by direct infection [8,10,16]. We show that inducible reprogramming in genetically homogenous cultures creates iDA neurons that are highly similar to primary midbrain DA neurons, both in their molecular and functional characteristics. Additionally, we show the direct lineage reprogramming of iDA neurons from cells of the hematopoietic lineage using this system, demonstrating that abundant and readily accessible somatic cell types, such as peripheral blood cells, are amenable to direct lineage reprogramming and can give rise to functional iDA neurons. Taken together, our results suggest that inducible gene expression in a genetically homogeneous system enables the efficient production of high quality iDA neurons, which can greatly facilitate the application of these cells in PD disease modeling, drug screening, and, ultimately, cell replacement therapy.

2. Results

2.1. Generation of an expression system for the generation of genetically homogenous iDA neurons

Previously, we and others have shown that both mouse and human fibroblasts can be directly reprogrammed into iDA neurons through the viral transduction of several transcription factors, such as Ascl1, Pitx3, Nurr1, Lmx1a, Foxa2 and EN1 [3–5,7]. Among these factors, the combined activity of Ascl1 and Pitx3 is sufficient to facilitate conversion into a cell with DA neuronal identity (and activation of an endogenous *Pitx3-eGFP* knock-in reporter allele), while ectopic expression of additional factors is thought to be involved in the further maturation of 2 factor-induced *Pitx3-eGFP*$^{+}$ iDA neurons.

We asked if the efficiency and quality of iDA neuron generation could be improved using a genetically homogenous inducible reprogramming system. We first generated mouse embryonic stem (ES) cells containing both a reverse tetracycline transactivator (M2rtTA) and a *phosphoglycerate kinase 1* (*pgk1*) promoter-driven puromycin resistance gene targeted to the *ROSA26* locus (*ROSA26-M2rtTA*) in addition to an enhanced green fluorescent protein (*eGFP*) (in the Web version)gene targeted to the endogenous *Pitx3* locus. These ES cells were next infected with doxycycline (dox)-inducible lentiviruses encoding the transcription factors (Fig. 1A). Previously, we reported that the viral transduction of a 6-factor combination (Ascl1, Pitx3, Nurr1, Lmx1a, EN1, and Foxa2) could generate iDA neurons that closely resemble midbrain DA neurons [6]. However, when we prepared ES cells harboring all 6 factors, they exhibited promiscuous differentiation even in the absence of dox, precluding their maintenance over multiple passages (data not shown). Thus, we removed the non-requisite factors EN1 and Foxa2 from the 6-factor combination, generating *Pitx3-eGFP* ES cells harboring a 4-factor combination (Ascl1, Pitx3, Nurr1 and Lmx1a). We generated several unique clones of these 4-factor ES cells (J1, J2, J3), all of which were stable and could be maintained in culture in the absence of dox for more than 20 passages (Fig. 1B). Hereafter, we refer to these cells as *Pitx3-eGFP-TRE-4F*.

Southern blot analysis probing for proviral integration of Ascl1, Pitx3, Lmx1a and Nurr1 vectors showed that each of the three ES cell lines were independent clones carrying approximately 10 proviral integrations for each gene (Fig. 1D). These *Pitx3-eGFP-TRE-4F* ES cells were GFP negative in the absence of dox (not shown), and all of the ES cell colonies showed morphology characteristic of mouse ES cells (Fig. 1B). The pluripotency of these ES cells was confirmed by the expression of marker genes, including *Oct4*, *Nanog*, and *Sox2*, and neuronal genes, including *TH*, *Tuj1 and Brn2/4*, were not expressed. Additionally, no differences in the expression of these genes were observed between the ES cells (Fig. 1C), demonstrating the inducible factors has no detrimental consequences for the ability of the ES cells to maintain pluripotency, nor does it result in any aberrant expression of neuronal-lineage genes in the absence of Dox stimulation. To generate inducible somatic cells, we injected these ES cell lines into blastocysts and generated chimeras composed of *Pitx3-eGFP-TRE-4F* somatic cells as well as host blastocyst-derived cells. Mouse embryonic fibroblasts (MEF) were prepared from these chimeras and treated with puromycin to select against cells derived from the host blastocyst by virtue of the constitutively active puromycin resistance cassette at the *ROSA26* locus.

To assess inducible expression of the reprogramming factors in *Pitx3-eGFP-TRE-4F* MEFs, we performed transgene-specific quantitative RT-PCR. We detected robust dox-dependent factor expression in all three *Pitx3-eGFP-TRE-4F* MEF lines, with J1 giving the most robust expression (Sup. Fig. 1 A–D). Therefore, we used inducible fibroblasts from *Pitx3-eGFP-TRE-4F* J1 for subsequent experiments. Taken together, these results indicated that transgene expression was strictly dependent on the presence of the drug, with little to no leaky expression as no viral transcripts were detected in the absence of dox.

2.2. Efficient direct lineage reprogramming of Pitx3-eGFP-TRE-4F fibroblasts into iDA neurons

We next assessed the reprogramming activity of *Pitx3-eGFP-TRE-4F* MEFS in response to dox treatment. The addition of dox led to dramatic morphological changes and efficient generation of cells resembling DA neurons (Fig. 2A and B). Seven days after dox induction, most fibroblasts in the culture appeared to be TH + iDA neurons, and immunofluorescence demonstrated that iDA neurons had reactivated the DA neuronal markers TH, DAT, Tuj1, AADC, VMAP2, and Girk2 (Fig. 2C and Sup. Fig. 2C). We observed the highest induction of TH + iDA neurons in *Pitx3-eGFP-TRE-4F* J1 fibroblasts (Fig. 2D). The reprogramming efficiencies of the different

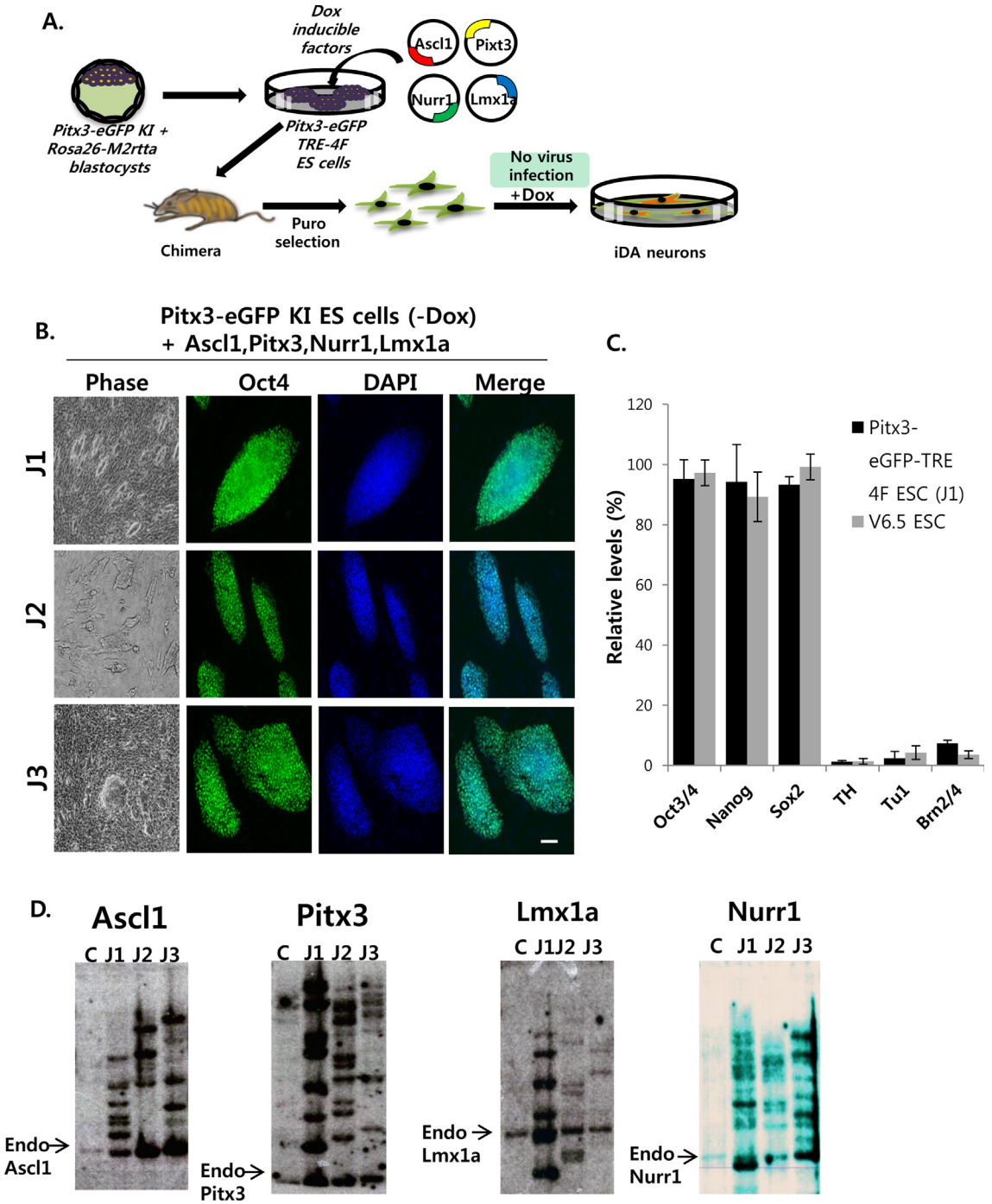

Fig. 1. (A) Schematic drawing representing the strategy used in this study for inducible direct lineage reprogramming into induced dopamine (DA) neurons. Induced dopaminergic (iDA) neurons were prepared from mouse somatic cells generated from Pitx3-eGFP knock-in (KI) ES cells carrying specific combinations of doxycycline (dox)-inducible factors (*Pitx3-eGFP-TRE-4F*). (B) Bright field image and immunofluorescence staining of *Pitx3-eGFP-TRE-4F* ES cells for the pluripotency marker Oct4. Scale bar = 50 μm (C) quantitative RT-PCR for the expression of endogenous pluripotency genes, Oct4, Nanog and Sox2 and neuronal genes TH, and Tuj1 in control mouse ES cells (V6.5) and *Pitx3-eGFP-TRE-4F* ES cells harboring Aslc1, Nurr1, Lmx1a and Pitx3. Data represent the mean ± SEM, no significant differences between control ES cells and factor infected Pitx3 ES cells. (D) Southern blot analysis of mouse ES cells (V6.5) and *Pitx3-eGFP-TRE-4F* ES cells for proviral integrations of BamHI digested genomic DNA using P32-labeld DNA probes against Ascl1, Pitx3, Lmx1a and Nurr1.

iDA neurons appeared to be positively correlated with transgene expression levels, as shown in Fig. 1D. We also quantified the expression of DA neuron-related genes in these cultures. Seven days of dox-induction in *Pitx3-eGFP-TRE-4F* J1 cultures resulted in a significant increase in the expression of endogenous TH, AADC, DAT, EN1, MAPT, and VMAT2, and these levels were similar to those observed in the primary dopamine neurons of the midbrain, which express high levels of TH, AADC, DAT, and EN1, and low levels of FAP, relative to fibroblasts, suggesting that inducible iDA neurons are highly similar to endogenous DA neurons in terms of marker gene expression (Fig. 2E and Sup. Fig. 2A). Additionally, specific induction of pan-neuronal genes, such as MAPT, and NEFL, was also observed in iDA neurons, whereas the expression of fibroblast genes was significantly downregulated in iDA neurons (Sup.

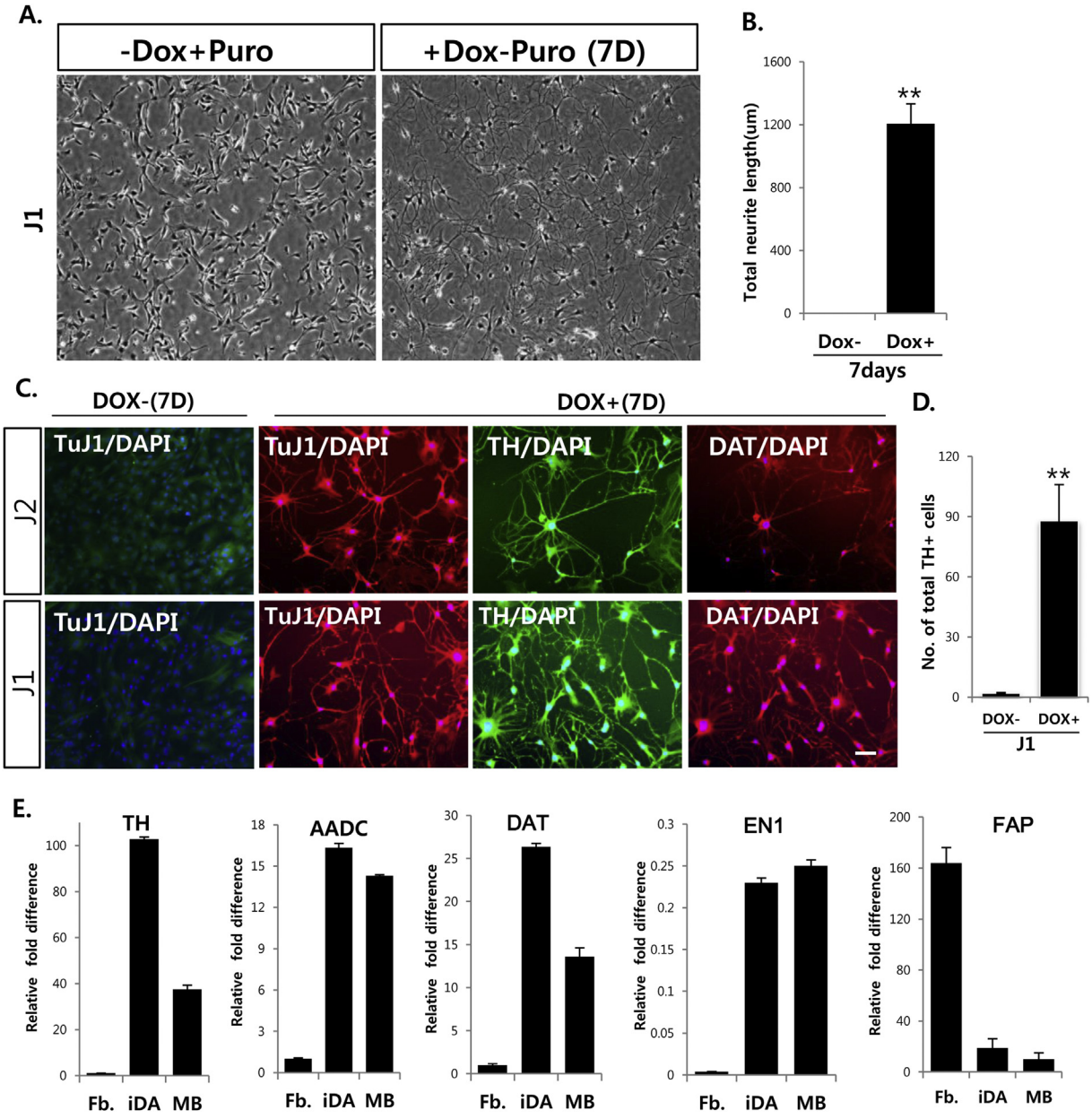

Fig. 2. (A) Phase contrast images of J1 inducible fibroblasts (left image), and iDA neurons 7 days after dox treatment (right image). (B) Average neurite length of iDA neurons derived from J1 fibroblasts 7 days after dox treatments. (C) Immunofluorescence images of iDA neurons derived J1 and J2 fibroblasts stained with the indicated markers. iDA neurons from *Pitx3-eGFP-TRE-4F* mouse embryonic fibroblasts (MEFs) J1 and J2 generated 7 days after dox treatment. Scale bar = 50 μm. (D) Number of total TH positive cells per well 7 days after dox treatment in the inducible *Pitx3-eGFP-TRE-4F* fibroblasts J1. Three independent chimeras of three sets each were performed with 10 visual fields per set; data represent the mean ± SEM, *Student's t-test*, $^{**}p < 0.01$. (E) Quantitative RT-PCR showing the expression of DA neuronal and fibroblasts marker genes in fibroblasts, iDA neurons and primary mouse midbrain (MB) (postnatal day 1).

Fig. 2A). Importantly, we were able to detect dopamine release in the context of high potassium (56 mM)-induced depolarization in iDA neurons (Sup. Fig. 2B), as expected for functional DA neurons that produce and release dopamine.

We next sought to compare the efficiency and reproducibility of the *Pitx3-eGFP-TRE-4F* system with that of direct infection. *Pitx3-eGFP* fibroblasts were directly infected with inducible lentiviruses encoding Aslc1, Pitx3, Nurr1 and Lmx1a and scored for TH + cells on day 10 after dox induction. Five independent experiments show significantly lower efficiency and higher variability in the generation of TH + iDA neurons by direct lentiviral infection compared to our *Pitx3-eGFP-TRE-4F* system (Fig. 3A). Moreover, we found that endogenous DA-specific gene expression (including TH, Tuj1, VMAT2, AADC, and DAT) was much more robust in *Pitx3-eGFP-TRE-4F* iDA cultures compared to those arising from direct infection (Sup. Fig. 3A–C).

The homogeneity of *Pitx3-eGFP-TRE-4F* also enables more precise characterization of the kinetics of cell fate conversion. To test the minimum requirements for exogenous transgene expression in iDA generation, we exposed *Pitx3-eGFP-TRE-4F* J1 fibroblasts to dox for various periods of time between 1 and 20 days and then stained the cells to examine TH expression (Fig. 3B). Remarkably, TH + iDA neurons with neuronal morphology appeared in *Pitx3-eGFP-TRE-4F* fibroblasts exposed to dox for as little as 1 day, while no TH + iDA neurons were detected in the cultures that were not exposed to dox or were treated for less than 1 day (Fig. 3C). The number of iDA

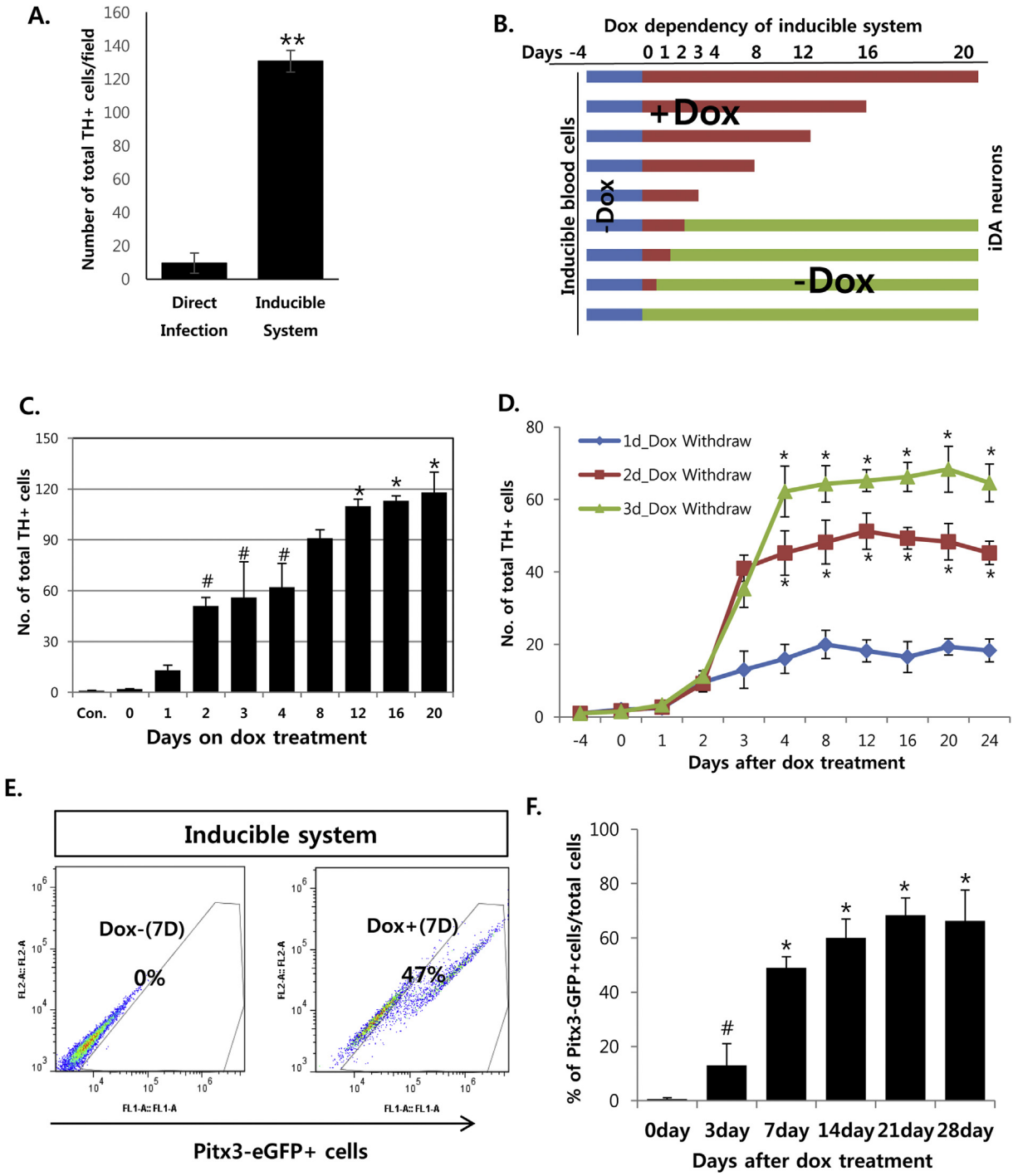

Fig. 3. (A) Comparison of the experimental variability in iDA neuron formation efficiency between direct infection and the inducible system. The number of total TH + cells per field from five independent experiments. Data represent the mean ± SEM, *Student's t-test*, $^{**}p < 0.01$. (B) Experimental scheme of the reprogramming kinetics experiment. *Pitx3-eGFP-TRE-4F* MEFs were cultured in the presence of dox (+dox) for the indicated times followed by dox withdrawal (-dox). (C) The number of total TH + iDA neurons in the culture on the indicated days is shown. The inducible cultures were maintained in the presence of dox for indicated number of days and the number of TH + iDA neurons were monitored at the indicated day. Data represent the mean ± SEM, *ANOVA test*, $^{*}p < 0.05$ compared to day 3, $^{\#}p < 0.05$ compared to day 1 (D) *Pitx3-eGFP-TRE-4F* MEFs were culture in the presence of dox for 1, 2 or 3 days, and the number of TH + iDA neurons was counted on the indicated day up to day 20. Data represent the mean ± SEM, ANOVA *test*, $^{*}p < 0.05$. (E) FACS analysis of eGFP induction from *Pitx3-eGFP-TRE-4F* MEFs (right panel) and viral infected fibroblasts (left panel) 7 days after dox treatment. (F) Reprogramming efficiency of the generated iDA neurons. FACS analysis for eGFP induction from *Pitx3-eGFP-TRE-4F* after 3, 7, 14, 21, and 28. Data represent mean ± SEM, ANOVA *test*, $^{\#}p < 0.05$ compared to the 0 day, $^{*}p < 0.05$ compared to the 3 day.

neurons increased with prolonged exposure to dox, plateauing after approximately 12 days of dox exposure, as measured by quantification of TH + iDA neurons. To examine the effect of exogenous reprogramming factor expression on iDA neurons, dox was withdrawn from the *Pitx3-eGFP-TRE-4F* cultures after 1, 2 or 3 days of exposure. The number of TH + iDA neurons was then assessed 20 days after the initial dox induction. We found that a small number of TH + iDA neurons from inducible fibroblasts appeared one day after dox treatment (Fig. 3D). Two days of dox treatment generated a significant increase in stable TH + iDA neurons with no apparent

loss of TH + cells during the period of dox withdrawal (Fig. 3D). Taken together, these results demonstrate that this inducible system can efficiently generate iDA neurons when cultured in the presence of dox and these iDA neurons are stably reprogrammed and independent of exogenous transgene expression. We further examined reprogramming efficiency by flow cytometry on day 0, 7, 14, 21 and 28 after dox induction. *Pitx3-eGFP-TRE-4F* iDA neurons were 47% GFP^{+} by day 7 (Fig. 3E), reaching a maximum of approximately 68% of total cells by day 28 (Fig. 3F), while viral-mediated infection generated approximately 4% of Pitx3-GFP + DA neurons (Sup. Fig. 4A). Taken together, these results indicate that the *Pitx3-eGFP-TRE-4F* system provides a more reproducible, homogenous, and efficient iDA conversion system compared to direct infection methods.

2.3. Inducible iDA neurons are highly similar to endogenous DA neurons

To further characterize *Pitx3-eGFP-TRE-4F* iDA neurons, we examined electrophysiological properties characteristic of functional *bona fide* DA neurons. iDA neurons were analyzed using whole-cell patch-clamp analysis at different points after dox

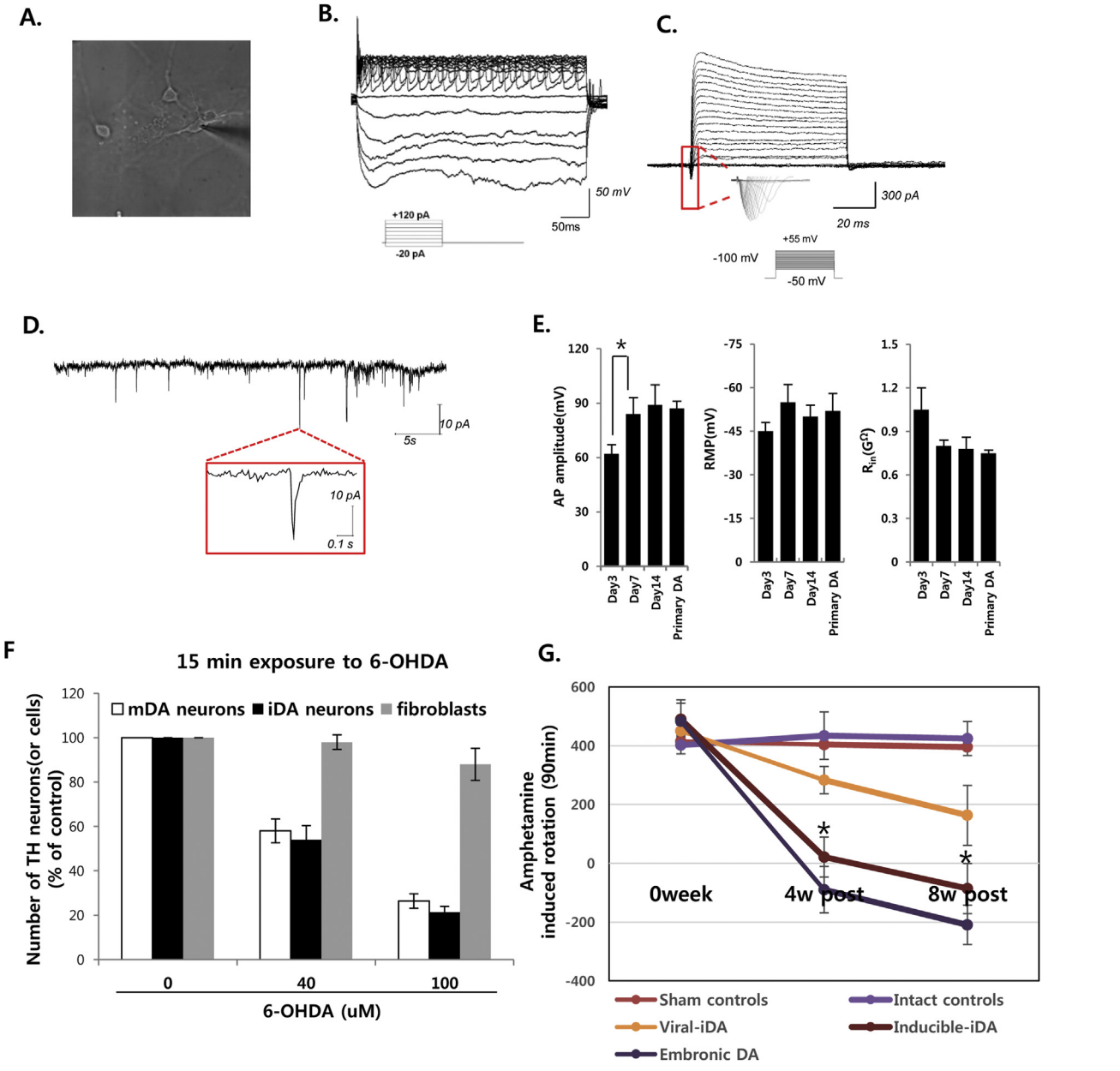

Fig. 4. (A) Example of electrophysiological recordings from iDA neurons with typical neuronal morphology. (B) Repetitive action potentials induced when increasing amounts of current were injected. Bottom traces represent current injections (−20 pA to +120 pA). (C) Voltage dependent membrane currents and depolarizing voltages step elicited fast inward sodium currents and slow inactivating outward potassium currents. (D) Spontaneous synaptic activity of the iDA neurons. (E) Quantification of membrane properties in inducible iDA neurons cells at 3, 7 and 14 days after dox treatment. Data are presented as the mean ± SEM, *Student's t-test*, $^{*}p < 0.05$. AP, action potential; Rin, membrane input resistances; RMP, resting membrane potential. (F) Data were quantified for 6-OHDA effects on primary DA neurons, iDA neurons and fibroblasts by counting the cells. The cells with neuronal morphologies were counted in the primary DA neuron and iDA neuronal cultures. 10 independent wells of plates were counted in triplicated sets of experiments. Data are presented as the mean ± SEM. (G) Amphetamine-induced (4 mg/kg) rotational behaviors for 90 min in 6-OHDA lesioned mice (intact controls, n = 10) prior to cell transplantation, and 4 and 8 weeks after the transplantation of viral (viral-DA) and inducible mediated Pitx3-eGFP + cells (inducible DA), control fibroblasts (sham controls), and primary embryonic midbrain Pitx3-eGFP + cells (Embryonic DA) into the lesioned striatum. Data represent mean ± SEM; ANOVA test, $^{*}p < 0.05$. (n = 11) lesioned mice for each group.

induction. 7 days after dox induction, the majority of iDA neurons elicited action potentials (14 out of 15 cells, Fig. 4A and B) in contrast to control fibroblasts, which were negative (data not shown). Furthermore, *Pitx3-eGFP-TRE-4F* iDA neurons also exhibited voltage-dependent ionic currents (Fig. 4C) and showed spontaneous synaptic activities (Fig. 4D). Three days after dox induction, the average resting membrane potential of inducible iDA neurons was −45.18 ± 5.3 mV (mean ± SEM, n = 14), the input resistance was 1.07 ± 0.47 GΩ (mean ± SEM, n = 14), and action potential amplitude was 64.26 ± 6.83 mV (mean ± SEM, n = 14), indicating the presence of well-developed Na channels and K channels in iDA neurons (Fig. 4E). By these parameters, *Pitx3-eGFP-TRE-4F* iDA neurons were indistinguishable from primary DA neurons (Fig. 4E).

To further examine the extent to which *Pitx3-eGFP-TRE-4F* iDA neurons are functionally analogous to primary DA neurons, we performed 6-hydroxydopamine (6-OHDA) response assays. Mitochondrial defects are implicated in Parkinson's disease, and 6-OHDA can directly lead to destruction of DA neurons via mitochondrial stress [17]. To examine effects of 6-OHDA on iDA neurons, we treated 7-day iDA neurons, primary DA neurons, and fibroblasts with various concentrations of 6-OHDA and assessed cell death. iDA neurons and primary neurons treated with 40 μM–100 μM of 6-OHDA responded identically, dying in a dose-dependent manner, in contrast to fibroblasts, which were largely resistant to 6-OHDA (Fig. 4F).

Ultimately, we tested the functional efficacy of *Pitx3-eGFP-TRE-4F* iDA neurons in a murine cell transplantation therapy model of Parkinsonism. Five days after dox treatment, Pitx3 GFP + iDA neurons were isolated by FACS and immediately implanted into the striatum of mice with 6-OHDA lesions that occurs with DA loss in the midbrain. Eight weeks after transplantation, the implanted Pitx3-eGFP + iDA neurons led to a significant reduction in amphetamine-induced rotation scores in 6-OHDA-lesioned mice (Fig. 4G and Sup. Fig. 5A–D). In contrast, transplantation of control cells infected with eGFP-expressing lentivirus did not show any rescue of the amphetamine-induced rotation (sham control). Additionally, to test whether the transplanted iDA neurons actually integrated into the host striatum, we performed the spontaneous exploratory forelimb use test. We observed no significant differences between the performance scores of the two groups, indicating that transplanted iDA neurons are not fully integrated into the host striatum but produce functional improvement by DA release (Sup. Fig. 5E) Together, these results validate the functional qualities of *Pitx3-eGFP-TRE-4F* iDA neurons, indicating that they are an appropriate platform for drug screening, suggesting that this strategy may provide a viable therapeutic cell source for cell replacement therapy in Parkinson's disease.

2.4. iDA neurons from hematopoietic lineages are also highly similar to endogenous iDA neurons

Previously, inducible systems for reprogramming to pluripotency have been used to determine whether different somatic cell types are permissive for iPS cell reprogramming [6,8,9]. Particularly, it has been shown that hematopoietic lineages are a readily accessible source of cells from patients that are amenable to reprogramming to pluripotency [9,18]. Because peripheral blood is the most accessible/least invasive cell source in the adult, we examined whether iDA neurons can be derived from peripheral mononuclear blood cells using the *Pitx3-eGFP-TRE-4F* system.

We isolated monocytes from the peripheral mononuclear blood cells of a *Pitx3-eGFP-TRE-4F*-J1 chimera using an Easysep mouse monocyte enrichment kit. The isolated monocytes were cultured using *in vitro* monocyte culture media with dox for 5 days. Five days after dox induction, the cells were transferred to N3 medium containing dox (Fig. 5A). Ten days later, reprogrammed iDA neurons were examined. Immunofluorescence staining showed that monocyte-derived iDA neurons uniformly expressed the DA markers TH and TuJ1 (Fig. 5B). We next analyzed DA neuron-related transcript levels in iDA neurons compared to primary DA neurons at the single cell level. Fifteen days after dox treatment, monocytes, Pitx3-GFP-positive iDA neurons and primary Pitx3-GEP + DA neurons were FACS sorted into single cells, and mRNA levels were analyzed using single cell real-time polymerase chain reaction (RT-PCR). Fig. 5C shows that monocyte-derived iDA neurons establish gene expression profiles highly similar to primary midbrain DA neurons (Fig. 5C). We observed some variability in the expression of these genes, which may be due to the small number of incomplete reprogrammed cells. The number of TH + iDA neurons and neurite lengths were significantly increased in the monocyte-derived iDA neurons (Fig. 5D and E). HPLC analysis revealed that monocyte-derived iDA neurons contain high levels of intracellular dopamine, which can be released into the extracellular medium upon stimulation with 50 mM KCl (Fig. 5F).

We next analyzed endogenous DA neuron-related transcript levels in iDA neurons compared to primary DA neurons at the single cell level. Fifteen days after dox treatment, monocytes, primary Pitx3-eGFP^{+} DA neurons, and monocyte-derived Pitx3-eGFP + *i*DA neurons were FACS-purified, and mRNA levels were analyzed using single cell qRT-PCR. Fig. 4C shows that monocyte-derived iDA neurons exhibit gene expression patterns that are highly similar to those in primary midbrain DA neurons. We also recorded the electrophysiological properties of monocyte-derived iDA neurons. Most of the analyzed iDA neurons showed action potentials when depolarized by current injections (Fig. 5G). Moreover, monocyte-derived iDA neurons generated fast inward Na currents and outward K currents (Fig. 5H). The average resting membrane potential and AP amplitude of iDA neurons were indistinguishable from those of primary midbrain DA neurons (Fig. 5I). Taken together, drug-induced, hematopoietic lineage-derived iDA neurons acquired functional properties that were highly similar to those of endogenous midbrain DA neurons.

3. Discussion

Parkinson's disease (PD) is characterized by a progressive loss of nigrostriatal dopamine caused by the degeneration of mesencephalic dopamine (DA) neurons. DA neurons, unlike many other cell types, have a limited capacity for self-repair and lack the ability to regenerate [19]. Therefore, identifying an abundant source of patient-specific DA neurons for disease modeling and potential cell-based therapy is of tremendous interest. The isolation and expansion of large numbers of somatic cells, such as fibroblasts, from patients offers a vast potential reservoir of target cells for directed reprogramming into genetically matched DA neurons [3]. The generation of functional neurons from abundant somatic cells by ectopic expression of factors opens a new avenue for the therapies in neurological disease [1]. Particularly, direct lineage reprogramming of somatic cells into DA neurons through the expression of reprogramming factors potentially provides a novel point of therapeutic intervention in PD [3,4,7]. However, iDA neurons generated by direct viral infection results in the inefficient generation of a genetically heterogeneous cell population with incomplete or variable reprogramming.

Here, we report the generation of a genetically homogenous system for the controlled expression of exogenous reprogramming factors. This system results in cultures of iDA neurons that are more efficiently generated in a robust and reproducible manner compared with direct infection, ultimately resulting in iDA neurons that are functionally indistinguishable from primary DA neurons.

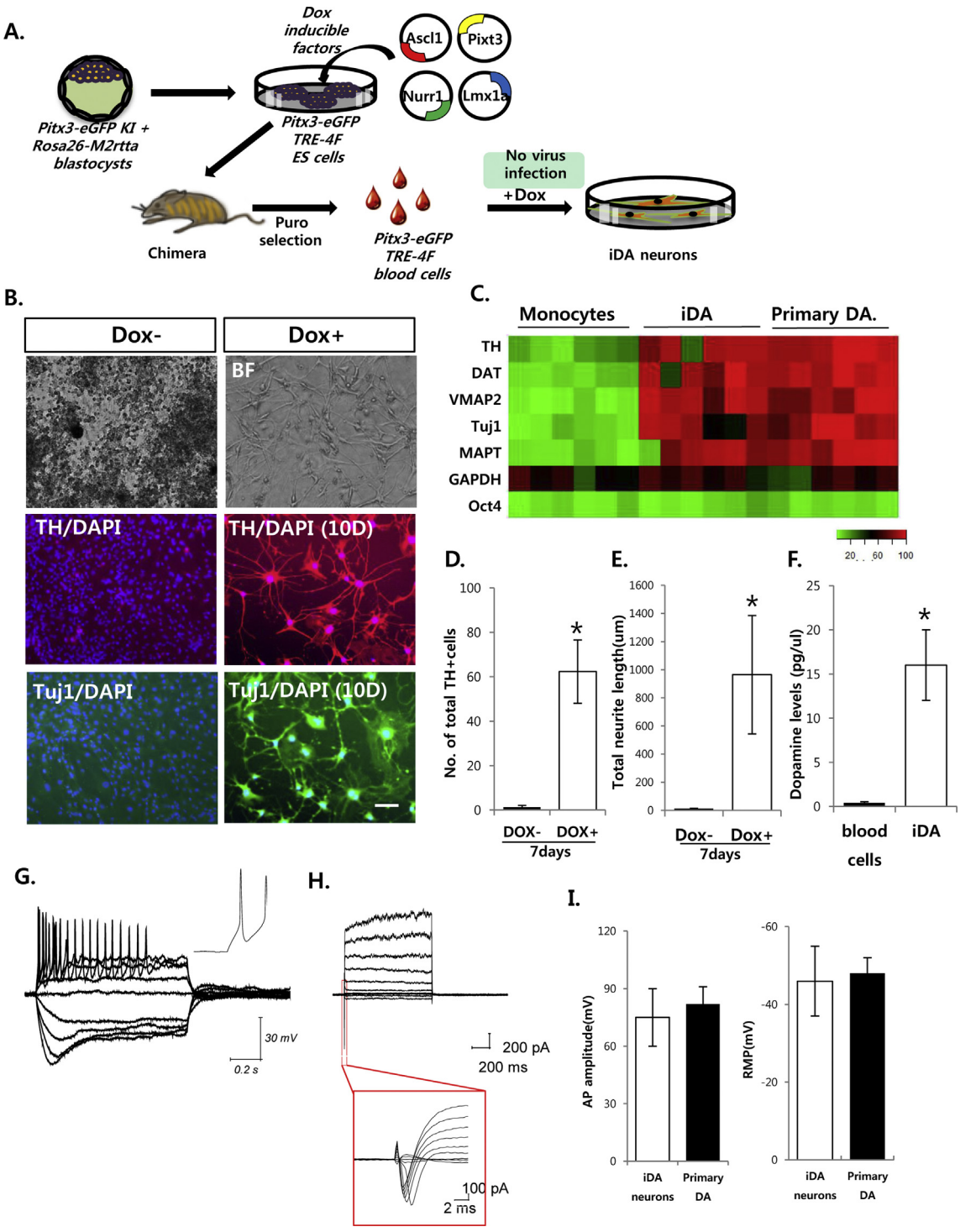

Fig. 5. (A) Schematic drawing representing the strategy used in this study for inducible direct lineage reprogramming into induced dopamine (DA) neurons from blood cells. The monocytes were isolated from the peripheral mononuclear blood cells from chimeric mice using an Easysep mouse monocyte enrichment kit. The isolated monocytes were cultured using *in vitro* monocyte culture media with dox for 5 days. (B) Representative images of inducible iDA neurons from monocytes in the presence and absence of dox for 7 days (top panel). Immunofluorescence staining of blood derived iDA neurons for DA neuron markers, TuJ1 and TH (middle and bottom panel). Scale bar = 50 μm (C) single cell gene expression profiling. Rows represent the evaluated genes and columns represent individual cells from monocytes, *Pitx3-eGFP-TRE-4F* iDA neurons and primary *Pitx3-eGFP*+ dopamine neurons. The heat map represents the relative expression of the indicated genes. (D) Number of TH + iDA neurons from *Pitx3-eGFP-TRE-4F* monocytes. (E) Total nitrite length of iDA neurons from *Pitx3-eGFP-TRE-4F* monocytes. (F) HPLC quantification of KCl induced dopamine release from *Pitx3-eGFP-TRE-4F* iDA neurons and *Pitx3-eGFP-TRE-4F* monocytes. Data represent mean ± SEM; three independent experiments were performed; *Student's t-test*, $^{*}p < 0.05$. (G) Representative action potentials generated from iDA neurons derived monocytes. (H) Voltage dependent membrane currents and depolarizing voltages step elicited fast inward sodium currents and slow inactivating outward potassium currents of blood derived iDA neurons. (I) Quantification of membrane properties in blood derived iDA neurons cells 7 days after dox treatment. Data are presented as the mean ± SEM. AP, action potential; RMP, resting membrane potential.

Previous studies reporting the generation of iDA neurons via direct viral infection resulted in reprogrammed cells that did not closely resemble the molecular features of endogenous midbrain DA neurons [3,4]. This result may be due to incomplete reprogramming in a large fraction of the heterogeneous infected cell population due to large variability in the copy number and in the proviral site of integration.

Recently, chemically induced transdifferentiation from mouse or human fibroblasts into different cell types has been reported to address these challenges [20]. Because small molecules can be used in place of transcription factors and improve reprogramming efficiency and quality, a chemical method appears to be the most promising method. In fact, Hu et al., recently showed that cocktails of small molecules can induce the conversion of human fibroblasts into neurons, demonstrating the feasibility of using transgene-free iNs in regenerative medicine [20]. Moreover, biomaterial approaches such as electrospun substrates or nano-patterned substrates have been shown to efficiently control cell fate changes in cell reprogramming [13,21,22]. These biomaterial approaches provide an opportunity to optimize the cellular microenvironment to alter the desired cellular behaviors, which eventually lead to cell reprogramming. Nevertheless, we found that the low yield of chemical-induced non-proliferative DA neurons and more systematic approach necessary to prepare the biomaterials limit the broad application of iDA neurons for regenerative medicine. In this regard, our system provides efficient and reproducible reprogrammed target cells with high similarity to their *bona fide in vivo* counterparts. The efficient and rapid direct conversion shown in the inducible system is likely the result of robust and homogenous reprogramming factor activation in comparison to chemical and biomaterials-mediated direct reprogramming. Consistent with this idea, it has recently been reported that reprogramming factor transduction using polycistronic vectors increases reprogramming efficiency in directly reprogrammed cells [23]. Furthermore, the efficient reprogramming that we observed in the inducible system is in agreement with previous reports of inducible reprogramming systems for the generation of induced pluripotent stem cells [8,16].

We also show that hematopoietic lineages can be directly reprogrammed into DA neurons. Previously, genetic lineage tracing experiments have shown that induced neurons can be derived from liver cells by the overexpression of ABM (Ascl1, Brn2 and Mytl1) factors [24]. Generation of iDA neurons from peripheral blood is of particular interest in regenerative medicine because peripheral blood is the most readily accessible and abundant adult tissue. Peripheral blood mononuclear cells underwent robust and rapid dox-induced reprogramming into functional iDA neurons. Thus, our results demonstrate direct cell fate conversion into iDA neurons from peripheral blood and also demonstrate the utility of our system for direct lineage reprogramming of various somatic cell types, such as blood, which are refractory to direct viral infection.

4. Conclusion

Genetically homogenous factor expression in the inducible iDA system shows highly reproducible kinetics and efficiencies. Therefore, the approach to establish a genetic homogenous factor expression system can be used to generate high quality iDA neurons from PD patients, providing a robust platform not only for screening potential therapeutic interventions but also for potential cell replacement therapies. Thus, the generation of high quality, functional DA neurons by direct lineage reprogramming has significant implications in disease modeling and therapeutic intervention for PD.

5. Methods and materials

5.1. Lentivirus generation & infection

VSVG-coated lentiviruses were generated in 293 cells as described previously (Kim et al., 2010). Viral supernatant were pools for 4 factor infections and Pitx3-eGFP KI ES cells were seeded 24 h before transduction. Three consecutive infections were performed on the Pitx3-eGFP KI ES cells and the ES cell colonies were picked based on morphology 3 day after the last infection. Infected ES cells were maintained and passaged according to standard mouse ESC protocols in the absence of doxycycline.

5.2. Blastocyst injection & fibroblast preparation

We generated embryonic stem (ES) cells containing both an M2rtTA and a *pgk1* promoter-driven puromycin resistant gene targeted to the *ROSA26* locus in addition to an *eGFP* gene targeted to the endogenous *Pitx3* locus by mating a Pitx3-eGFP knock-in mouse with a ROSA26-M2rtta mouse. After the reprogramming factors were delivered into these ES cells by infection, Pitx3-eGFP KI ES cells were injected into B6XDBA F2 host blastocysts as describe previously [6]. Briefly, superovulated female B6D2F1 mice (7–8 weeks old) were mated to B6D2F1 stud males, and fertilized embryos were collected from oviducts. The injected zygotes were cultured in KSOM with amino acids at 37 °C under 5% CO_2 in air until blastocyst stage by 3.5 days. Factor infected Pitx3-GFP + KI ES cells were injected into the blastocysts in M2 medium (Sigma). 15–25 blastocysts were transferred into the uterus of pseudo-pregnant ICR females at 2.5 dpc. Mouse embryonic fibroblasts (MEF) were prepared from these chimeras (E13.5) and treated with puromycin to select against cells derived from the host blastocyst by virtue of the constitutively active puromycin resistance cassette at the *ROSA26* locus. Fibroblasts were treated with dox followed by a change to neural culture medium (N3 media (Vierbuchen et al., 2010) supplemented with Shh and FGF8). Fresh neural culture medium with dox was added every other day for the desired time points after dox treatment.

5.3. Southern blot analysis

Genomic DNA (15 μg) was digested with the indicated restriction enzymes. Electrophoresis and transfer was performed according to standard procedures. The blots were hybridized to radioactively labeled probes against Ascl1, Pitx3, Nurr1 and Lmx1a. V6.5 ESCs were used as negative controls for determining background and endogenous bands.

5.4. Cell culture

For MEF isolation, the head containing the spinal cord, dorsal root ganglia and all internal organs were removed from Pitx3-eGFP KI E13.5 embryos. The remaining tissue was manually dissociated and incubated in 0.25% trypsin (Sigma) for 10–15 min to make single cells. The cells from each embryo were plated onto a 15-cm tissue culture dish in MEF media. The cells were grown at 37 °C for 3–4 days until confluent and then frozen. TTFs were isolated from *Pitx3-eGFP-TRE-4F* chimeric mice. Tail clips from adult heterozygote *Pitx3-eGFP-TRE-4F* mice (3 week old) were removed using surgical scissors. Tail clips were rinsed in ethanol, washed with PBS, and then dissociated using scissors and incubated with 0.25% trypsin for 10–15 min. TTFs were cultured in mouse embryonic fibroblasts (MEFs) media (DMEM; Invitrogen) containing 10% fetal bovine

serum (FBS; Hyclone), β-mercaptoethanol (Sigma–Aldrich), non-essential amino acids, sodium pyruvate and penicillin/streptomycin (Invitrogen) until confluent and passaged once prior to being pooled and frozen down for further use. After thawing, the cells were cultured on 15-cm plates and allowed to become confluent before being split using 0.25% trypsin onto plates for infections. The Easysep mouse monocyte enrichment kit (StemCell Technology, Cat:191971) was used for the isolation of mouse monocytes from peripheral mononuclear blood cells. Monocytes were maintained in RPMI1640 medium (Gibco BRL) supplemented with 10% heat-inactivated FCS, 0.03% L-glutamine, 100 mg/ml streptomycin, 100 mg/ml penicillin, 1 mM non-essential amino acids, 1 mM sodium pyruvate and 0.02 mM 2-mercaptoethanol (Invitrogen).

5.5. Flow cytometry

All flow cytometry was performed on an Accuri instrument (Becton–Dickinson). Data were analyzed with FlowJo software (TreeStar). Briefly, cells were dissociated with trypsin for 5 min and single cells were then pelleted, resuspended in ice-cold 4% paraformaldehyde, and incubated for 10 min at 4 °C. The cells were washed twice, resuspended in FACS buffer and then analyzed.

5.6. Immunocytochemistry

Cells were fixed in 4% paraformaldehyde in PBS and immunostained according to standard protocols using the following primary antibodies: TH (Pel-freez); Tuj1 (Sigma), MAP2 (Sigma), DAT (Chemicon), AADC (Protos Biotech), Pitx3 (Zymed) eGFP (Abcam), Oct4 (Santa Cruz) and appropriate fluorescent secondary antibodies (Invitrogen).

5.7. Quantitative RT-PCR

Total RNA was isolated using an RNeasy Kit (QIAGEN). One microgram of DNase treated RNA was reverse transcribed using a First Strand Synthesis kit (Invitrogen). Quantitative RT-PCR analysis was performed in triplicate using 1/50 of the reverse transcription reaction in an ABI Prism 7000 (Applied Biosystems, Foster City, CA) with Platinum SYBR green qPCR SuperMix (Invitrogen). Gene expression analysis for ES and neuronal markers was performed by RT-PCR. PCR primer sequences are available upon request.

5.8. Dopamine determination by reversed phase HPLC

Samples were sent to CMN/KC Neurochemistry Core Lab at Vanderbilt University for HPLC analysis. Detailed procedures were described previously [3]. Briefly, dopamine release in iDA neurons were incubated in HBSS containing 56 mM KCl for 15 min for stimulation and then lysed with 0.1 M perchloric acid with Na/meta-bisulfate. Catecholamines were determined by a specific HPLC assay utilizing an Antec Decade II electrochemical detector. Samples of the supernatant were injected using a Water 717 + autosampler onto a Phenomenex Nucleosil (5u, 100A) C18 HPLC column (150 × 4.60 mm). Analytes were eluted with a mobile phase consisting of 89.5% 0.1 M TCA, 10–2 M sodium acetate, 10–4 M EDTA and 10.5% methanol. Using this HPLC solvent, analytes were observed in the following order: DOPAC, dopamine, and HVA. HPLC control and data acquisition were managed by Waters Empower software. Total protein for each sample was determined using the Peirce BCA protein assay.

5.9. Neurotoxicity assay

One day prior to the neurotoxicity assay, medium with growth factor was replaced with DMEM:F12/N2 (-antioxidant) medium alone. 6-OHDA was freshly prepared and the entire experiment was conducted in the dark. The cells were treated with 6-OHDA for 7 days and were then induced with dox for 24 h prior to fixation with 4%PFA. The fixed cells were immunostained according to standard protocols with the indicated antibodies.

5.10. Electrophysiology

For electrophysiological recordings, cells were grown on 12 mm glass coverslips and transferred to recording medium containing the extracellular solution (in mM): 130 NaCl, 4 KCl, 2 $CaCl_2$, 1 $MgCl_2$, 10 HEPES, 10 glucose (pH 7.35, 325 mOsm). Patch pipettes were filled with the following intracellular solution (in mM): 110 potassium gluconate, 20 KCl, 2 Mg-ATP, 10 sodium phosphocreatine, 1.0 EGTA, 0.3 GTP-Tris, and 20 HEPES (pH 7.25, 320 mOsm). Electrodes were fabricated from borosilicate capillary glass tubing (Warner Instruments) with a capillary glass puller (Sutter Instruments). After establishing whole-cell mode, the cell membrane capacitance and series resistance were compensated to 75% electronically using a patch clamp amplifier (Axopatch 200B; Molecular Devices). Data generation and acquisition were performed using pClamp10 software on an IBM computer equipped with an analog-to digital converter (Digidata 1440A; Axon Instruments). Recordings were conducted on the neuron-like morphology including elevated cell bodies and the presence of branched and neurites. Current injection protocol steps were applied ranging from −100 pA to +120 pA.

5.11. Cell transplantation

All animal experiments were performed according to the guidelines which were approved by the committee on animal care at Dongguk University animal center. For the generation of mouse model of Parkinson's disease, BL6C57 male mice (8week old) were anesthetized with Avertin, and 6OHDA was injected unilaterally into the midbrain region (SN) (AP: −3.1 mm; ML: ±1.1 mm; DV: −4.4 mm). 4 weeks after 6OHDA lesioned, the mice were injected with Amphetamine HCl (Sigma, 4 mg/kg i.p. injection) and amphetamine-induced turning behavior was assessed. Mice exhibiting net clockwise turns were lesioned in the left striatum, while mice exhibiting net counter-clockwise turns were lesioned in the right striatum (ipsilateral). Five days after dox treatment in to the culture, inducible Pitx3 GFP + cells were detached and sorted by FACS. Isolated Pitx3-eGFP + iDA cells were immediately resuspended in N3AA medium containing BDNF, GDNF and Boc-Asp. fluoromethyl ketone (BAF, Sigma) at a density of about 20,000 cells per ul. Mice were grafted into the lesioned striatum (AP: +0.4 mm; ML: ±1.5 mm; DV: −2.8 mm) with 3ul of cell suspension. Amphetamine-induced rotational behavior was measured again at 4 and 8 weeks after grafting. The number of clockwise and counter-clockwise turns was counted and expressed as the number of net rotations per 90 min to the hemisphere. Forelimb use during exploratory activity was analyzed by videotaping mouse in a transparent cylinder (20 in cm diameter and 30 cm in height) for 5 min. Scoring was done by an experimenter blinded to the condition of the animal and behavior was quantified by determining the occasions when the unimpaired (ipsilateral) forelimb was used as a percentage of total number of limb use observations on the wall; the occasions when the impaired forelimb was used as a percentage of total number of limb use observations on the wall; and the occasions when both forelimbs were used simultaneously as a percentage of total number of limb use observations on the wall.

5.12. Neurotoxicity assay

One day prior to neurotoxicity assay, medium with growth factor was replaced with DMEM:F12/N2 (-antioxidant) medium alone. 6-OHDA was freshly prepared and the entire experiment was done in the dark condition. 6OHDA was treated to the cells at day 7 dox induction and the treated cells were fixed with 4%PFA following 24-24 h after 6OHDA incubation without any disturbance. The fixed cells were immunostained according to standard protocols using the each antibodies.

5.13. Statistical analysis

Results are given as mean ± SEM. Where appropriate, statistical analysis was performed with an analysis of variance *(ANOVA)* test or *Student's t-test*. The null hypothesis was rejected at the $p < 0.05$ or 0.01 level.

Acknowledgments

This work was supported by the National Research Foundation funded by the Korea government, (NRF-2013R1A1A1058835), (NRF-2013M3A9B4076485), (NRF-2015 M3A9B4051064), Korea Health Technology R&D Project, Ministry of Health & Welfare (HI13C0540) and the Next-Generation BioGreen 21 Program, Rural Development Administration (PJ 01107701)

Appendix A. Supplementary data

Supplementary data related to this article can be found at http://dx.doi.org/10.1016/j.biomaterials.2015.09.002.

References

[1] T. Vierbuchen, A. Ostermeier, Z.P. Pang, Y. Kokubu, T.C. Südhof, M. Wernig, Direct conversion of fibroblasts to functional neurons by defined factors, Nature 463 (2010) 1035–1041.
[2] Y. Son Esther, K. Ichida Justin, J. Wainger Brian, S. Toma Jeremy, F. Rafuse Victor, J. Woolf Clifford, et al., Conversion of mouse and human fibroblasts into functional spinal motor neurons, Cell Stem Cell 9 (2011) 205–218.
[3] J. Kim, C. Su Susan, H. Wang, W. Cheng Albert, P. Cassady John, A. Lodato Michael, et al., Functional integration of dopaminergic neurons directly converted from mouse fibroblasts, Cell Stem Cell 9 (2011) 413–419.
[4] M. Caiazzo, M.T. Dell/'Anno, E. Dvoretskova, D. Lazarevic, S. Taverna, D. Leo, et al., Direct generation of functional dopaminergic neurons from mouse and human fibroblasts, Nature 476 (2011) 224–227.
[5] U. Pfisterer, A. Kirkeby, O. Torper, J. Wood, J. Nelander, A. Dufour, et al., Direct conversion of human fibroblasts to dopaminergic neurons, Proc. Natl. Acad. Sci. 108 (2011) 10343–10348.
[6] J. Kim, C.J. Lengner, O. Kirak, J. Hanna, J.P. Cassady, M.A. Lodato, et al., Reprogramming of postnatal neurons into induced pluripotent stem cells by defined factors, Stem Cells 29 (2011) 992–1000.
[7] X. Liu, F. Li, E.A. Stubblefield, B. Blanchard, T.L. Richards, G.A. Larson, et al., Direct reprogramming of human fibroblasts into dopaminergic neuron-like cells, Cell Res. 22 (2012) 321–332.
[8] M. Wernig, C.J. Lengner, J. Hanna, M.A. Lodato, E. Steine, R. Foreman, et al., A drug-inducible transgenic system for direct reprogramming of multiple somatic cell types, Nat. Biotech. 26 (2008) 916–924.
[9] J. Hanna, S. Markoulaki, P. Schorderet, B.W. Carey, C. Beard, M. Wernig, et al., Direct reprogramming of terminally differentiated mature B lymphocytes to pluripotency, Cell 133 (2008) 250–264.
[10] N. Maherali, T. Ahfeldt, A. Rigamonti, J. Utikal, C. Cowan, K. Hochedlinger, A high-efficiency system for the generation and study of human induced pluripotent stem cells, Cell Stem Cell 3 (2008) 340–345.
[11] S. Friling, E. Andersson, L.H. Thompson, M.E. Jönsson, J.B. Hebsgaard, E. Nanou, et al., Efficient production of mesencephalic dopamine neurons by Lmx1a expression in embryonic stem cells, Proc. Natl. Acad. Sci. 106 (2009) 7613–7618.
[12] C. Tian, Y. Li, Y. Huang, Y. Wang, D. Chen, J. Liu, et al., Selective generation of dopaminergic precursors from mouse fibroblasts by direct lineage conversion, Sci. Rep. 5 (2015) 12622.
[13] M. Maldonado, L.Y. Wong, C. Echeverria, G. Ico, K. Low, T. Fujimoto, et al., The effects of electrospun substrate-mediated cell colony morphology on the self-renewal of human induced pluripotent stem cells, Biomaterials 50 (2015) 10–19.
[14] A. Sánchez-Danés, A. Consiglio, Y. Richaud, I. Rodríguez-Pizà, B. Dehay, M. Edel, et al., Efficient generation of A9 midbrain dopaminergic neurons by lentiviral delivery of LMX1A in human embryonic stem cells and induced pluripotent stem cells, Hum. Gene Ther. 23 (2012) 56–69.
[15] S. Baek, X. Quan, S. Kim, C. Lengner, J.-K. Park, J. Kim, Electromagnetic fields mediate efficient cell reprogramming into a pluripotent state, ACS Nano 8 (2014) 10125–10138.
[16] D. Hockemeyer, F. Soldner, E.G. Cook, Q. Gao, M. Mitalipova, R. Jaenisch, A drug-inducible system for direct reprogramming of human somatic cells to pluripotency, Cell Stem Cell 3 (2008) 346–353.
[17] A.-R. Doo, S.-N. Kim, D.-H. Hahm, H. Yoo, J.-Y. Park, H. Lee, et al., Gastrodia elata Blume alleviates L-DOPA-induced dyskinesia by normalizing FosB and ERK activation in a 6-OHDA-lesioned Parkinson's disease mouse model, BMC Complement. Altern. Med. 14 (2014) 107.
[18] S. Eminli, A. Foudi, M. Stadtfeld, N. Maherali, T. Ahfeldt, G. Mostoslavsky, et al., Differentiation stage determines potential of hematopoietic cells for reprogramming into induced pluripotent stem cells, Nat. Genet. 41 (2009) 968–976.
[19] J. Kim, K. Inoue, J. Ishii, W.B. Vanti, S.V. Voronov, E. Murchison, et al., A MicroRNA feedback circuit in midbrain dopamine neurons, Science 317 (2007) 1220–1224.
[20] T. Lin, S. Wu, Reprogramming with small molecules instead of exogenous transcription factors, Stem Cells Int. 2015 (2015) 794632.
[21] J. Yoo, M. Noh, H. Kim, N.L. Jeon, B.-S. Kim, J. Kim, Nanogrooved substrate promotes direct lineage reprogramming of fibroblasts to functional induced dopaminergic neurons, Biomaterials 45 (2015) 36–45.
[22] J. Yoo, J. Kim, S. Baek, Y. Park, H. Im, J. Kim, Cell reprogramming into the pluripotent state using graphene based substrates, Biomaterials 35 (2014) 8321–8329.
[23] R. Wada, N. Muraoka, K. Inagawa, H. Yamakawa, K. Miyamoto, T. Sadahiro, et al., Induction of human cardiomyocyte-like cells from fibroblasts by defined factors, Proc. Natl. Acad. Sci. 110 (2013) 12667–12672.
[24] S. Marro, P. Pang Zhiping, N. Yang, M.-C. Tsai, K. Qu, Y. Chang Howard, et al., Direct lineage conversion of terminally differentiated hepatocytes to functional neurons, Cell Stem Cell 9 (2011) 374–382.